TABLE 2 Read Range of the Tag with the Proposed Antenna

Platform	30 dBm	27 dBm	24 dBm
Free space	3.3 m	2.4 m	1.3 m
Metal plate (0.2 m by 0.2 m)	3.6 m	2.7 m	1.7 m

cannot be made due to the limitation of the reader. However, according to earlier discussion, we can expect that this antenna will work well in the world-wide UHF RFID band.

4. CONCLUSION

A novel patch antenna which consists of four synchronous subpatches that resonates at four consecutive frequencies and inductively fed by a loop is designed and tested. The impedance is well matched to the RFID chip within the whole frequency band worldwide, and the gain is stable within the band. The read range is acceptable for most applications. Furthermore, the simple structure, small size and low-profile features make the antenna low cost and generally usable. Therefore, the proposed antenna has a great potential for mass applications of universal platform-tolerant tags.

ACKNOWLEDGMENTS

The work is supported by Hong Kong R&D center for Logistics and Supply Chain Management Enabling Technologies. The authors thank Dr. Zhi-Ning Chen for useful feedback and Dr. Hai-Long Zhu for antenna fabrication and testing.

REFERENCES

1. D.M. Dobkin, The RF in RFID: Passive UHF RFID in Practice, Elsevier Inc., 2008.
2. G. Marrocco, The art of UHF RFID antenna design: Impedance-matching and size-reduction techniques, IEEE Trans Antennas Propag Mag 50 (2008).
3. K.V.S. Rao, P.V. Nikitin, and S.F. Lam, Antenna design for UHF RFID tags: A review and a practical application, IEEE Trans Antennas Propag 53 (2005).
4. H. Kwon and B. Lee, Compact slotted planar inverted-F RFID tag mountable on metallic objects, Electron Lett 41 (2005).
5. M. Hirvonen, P. Pursula, K. Jaakkola, and K. Laukkanen, Planar inverted-F antenna for radio frequency identification, Electron Lett 40 (2004).
6. B. Yu, S.J. Kim, B. Jung, F.J. Harackiewicz, and B. Lee. RFID tag antenna using two shorted microstrip patches mountable on metallic objects, Microwave Opt Technol Lett 49 (2007).
7. B. Lee and B. Yu, Compact structure of UHF band RFID tag antenna mountable on metallic objects, Microwave Opt Technol Lett 50 (2008).
8. J. Dacuna and R. Pous, Low-profile patch antenna for RF identification applications, IEEE Trans Microwave Theory Techol 57 (2009), 1406–1410.
9. P.H. Yang, J.Z. Huang, W.C. Chew, and T.T. Ye, Design of compact and resuable platform-tolent RFID tag antenna using a novel feed method, Asia-Pacific Microwave Conference, 2009.
10. Z.N. Chen, X.M. Qing, and H.L. Chung, A universal UHF RFID reader antenna, IEEE Trans Microwave Theory Technol 57, 1275–1282.
11. L. Xu, B.J. Hu and J. Wang, UHF RFID tag antenna with broadband characteristic, Electron Lett 44 (2008).
12. C. Sahin, and D.D. Deavours, Wideband microstrip RFID tag: Theory and design, IEEE AP-S Internationl Antennas Propagation Symposium, 2009.
13. C. Cho, I. Park, and H. Choo, Design of a circularly polarized tag antenna for increased reading range, IEEE Trans Antennas Propag 57 (2009), 3418–3422.
14. L. Mo, H. Zhang, and H. Zhou, Broadband UHF RFID tag antenna with a pair of U slots mountable on metallic objects, Electron. Lett 44 (2008).
15. Z.N. Chen and M.Y.W. Chia, Broadband planar antennas: Design and applications, Wiley, Hoboken, NJ, 2006.
16. J.Z. Huang, P.H. Yang, W.C. Chew, and T.T. Ye, A compact broadband patch antenna for UHF RFID tags, Asia-Pacific Microwave Conference, 2009.
17. Available at: http://www.ccem.uiuc.edu/chew/fastant.html.
18. Available at: http://www.alientechnology.com.
19. K.D. Palmer and M.W. van Rooyen, Simple broadband measurements of balanced loads using a network analyzer, IEEE Trans Instrum Meas 55 (2006).
20. X. M. Qing, C.K. Goh, and Z.N. Chen, Impedance characterization of RFID tag antennas and application in tag co-design, IEEE Trans Antennas Propag 57 (2009), 1268–1274.

HEURISTIC UTD COEFFICIENTS FOR ELECTROMAGNETIC SCATTERING BY LOSSY CONDUCTING WEDGES

Daniela N. Schettino,[1] Fernando J. S. Moreira,[2] and Cássio G. Rego[2]

[1] ANATEL - National Agency for Telecommunications, Brasília, DF 70070-940, Brazil

[2] Department of Electronics Engineering, Federal University of Minas Gerais, Belo Horizonte, MG 31270-970, Brazil; Corresponding author: fernandomoreira@ufmg.br

Received 18 March 2010

ABSTRACT: *In this study, heuristic uniform theory of diffraction coefficients are suited to account for scattering by lossy conducting wedges. The novel heuristic solution is determined from other previously developed heuristic coefficients, combining their characteristics to improve the estimation of radiowave propagation in urban scenarios. Slope diffraction is also considered to account for double-diffracted fields in consecutive wedges. Maliuzhinets' coefficients provide base solutions to validate the novel formulation. The novel solution is then applied to the wave propagation in a typical urban scenario, and results are compared against measurements provided in the literature.*

Microwave Opt Technol Lett 52:2657–2662, 2010; View this article online at wileyonlinelibrary.com. DOI 10.1002/mop.25557

Key words: *diffraction coefficients; uniform theory of diffraction; radiowave propagation; nonperfectly conducting surfaces; slope diffraction*

1. INTRODUCTION

The numerical simulation of radiowave propagation in urban environments can be performed by different techniques. When site-specific analysis is required, the asymptotic solution given by the uniform theory of diffraction (UTD) [1] is largely used. The UTD was originally developed to evaluate the diffraction by perfectly conducting wedges. Since our aim is to analyze radiowave propagation in realistic scenarios, obstacles with finite conductivity must be considered.

Many heuristic solutions have been proposed to simulate the diffraction by wedges with finite conductivity. The solution presented in [2], based on the Maliuzhinets' formulation, is very precise but not practical for simulations with complex environments, since it depends on special functions with difficult numerical evaluation for arbitrary wedge angles. Aiming the same applicability and efficiency yield by the UTD for perfectly

conducting wedges, heuristic UTD coefficients were developed to estimate the diffraction by lossy obstacles [3–8]. In [3], Luebbers introduced the Fresnel reflection coefficients in the UTD diffraction coefficients, defining incidence and reflection angles according to the incident and diffracted rays. Although the solution is very practical, Luebbers' heuristic coefficients do not provide satisfactory results in deep shadow regions and are not reciprocal in relation to field direction of arrival, as they were derived for forward scattering analysis only. To improve the performance of Luebbers' coefficients in shadow regions, Holm derived heuristic coefficients based on the Fresnel-Kirchhoff theory, valid for wedges with arbitrary angles [4]. Although Holm's coefficients achieve better results in shadow regions, they still do not obey reciprocity. Aiming to turn Luebbers' coefficients into reciprocal ones, Aïdi and Lavergnat [5] heuristically proposed new angular definitions for the Fresnel reflection coefficients. However, Aïdi and Lavergnat's [5] coefficients still lack accuracy in some particular regions. The heuristic coefficients proposed in [6] aim the diffraction by structures having complex penetrable wedges, being difficult to be applyed in large urban scenarios. In [7], El-Sallabi and Vainikainen proposed heuristic diffraction coefficients and reflection angle definitions, which depend on the location of source and shadow boundaries and improve the results in the wedge lit region. Although good results were obtained, the approach is not very simple to use because the coefficients and angular definitions are quite complex and have many exceptions, depending on the wedge geometry and the positions of transmitter and receiver. In [8], the authors developed heuristic coefficients by substituting the angular definitions of [5] into Holm's coefficients [4], to make them reciprocal. However, the approach lacks accuracy in the lit region around the wedge.

All these heuristic coefficients present good results for some special situations, but not for arbitrary transmitter and receiver positions (i.e., for forward and back scattering), in both shadow and lit regions of the wedge. Thus, the objective of this study is to propose novel UTD heuristic coefficients suited to the analysis of the scattering by lossy wedges and, consequently, the characterization of radio channels. To estimate the usefulness and applicability of the proposed coefficients, scattering by arbitrary lossy wedges are investigated. The results obtained by the new heuristic coefficients are compared against those obtained from [3–5, 7], with Maliuzhinets' solutions adopted as reference. Results given by the new coefficients are also compared with path loss measurements performed in a typical urban scenario [9].

2. HEURISTIC UTD COEFFICIENTS FOR LOSSY CONDUCTING WEDGES

The heuristic diffraction coefficients introduced here are improvements over those presented in [3–8]. More specifically, the new coefficients are based on Holm's formulation [4], with angular definitions based on [3–5, 7]. The new coefficients are reciprocal and suited for the simulation of radiowave propagation in urban scenarios. The UTD electric field at the observer (Fig. 1) is defined as [1]:

$$E^d(O) = \overline{\overline{D}} \bullet E^i(W) A(s_\mathrm{d})\ e^{-jks_d} \tag{1}$$

where $\boldsymbol{E}^i(W)$ is the electric field incident at the wedge, $A(s_\mathrm{d})$ is the amplitude factor as defined in [1], s_d is the distance between wedge and observer, and $\overline{\overline{D}}$ is the dyadic diffraction coefficient, which has the following heuristic elements:

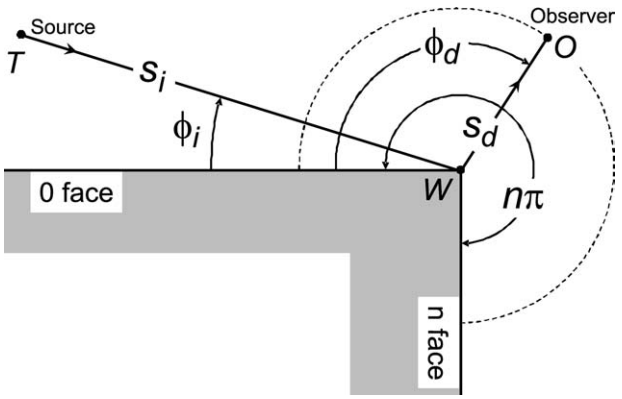

Figure 1 Geometry of the wedge with incident and diffracted rays

$$D_{\mathrm{s,h}} = G\left[H_{\mathrm{s,h}} D_1 + R_{\mathrm{s,h}}(\alpha_n) D_3 + D_2 + R_{\mathrm{s,h}}(\alpha_0) D_4\right] \tag{2a}$$

or

$$D_{\mathrm{s,h}} = G\left[D_1 + R_{\mathrm{s,h}}(\alpha_0) D_3 + H_{\mathrm{s,h}} D_2 + R_{\mathrm{s,h}}(\alpha_n) D_4\right] \tag{2b}$$

where D_i, for $i = 1, \ldots, 4$, are the usual UTD diffraction coefficients defined in [1], the factor $G = 1/2$ when grazing incidence occurs ($G = 1$ otherwise), and $R_{\mathrm{s,h}}(\alpha_0)$ and $R_{\mathrm{s,h}}(\alpha_n$ are the Fresnel reflection coefficients relative to the 0 and n wedge faces, respectively (Fig. 1). The subscripts s and h denote soft and hard polarizations, respectively, for which the Fresnel reflection coefficients are

$$R_\mathrm{s}(\alpha) = \frac{\sin\alpha - \sqrt{\hat{\varepsilon}_\mathrm{r} - \cos^2\alpha}}{\sin\alpha + \sqrt{\hat{\varepsilon}_\mathrm{r} - \cos^2\alpha}} \tag{3}$$

$$R_\mathrm{h}(\alpha) = \frac{\hat{\varepsilon}_\mathrm{r}\sin\alpha - \sqrt{\hat{\varepsilon}_\mathrm{r} - \cos^2\alpha}}{\hat{\varepsilon}_\mathrm{r}\sin\alpha + \sqrt{\hat{\varepsilon}_\mathrm{r} - \cos^2\alpha}} \tag{4}$$

where $\hat{\varepsilon}_\mathrm{r} = \varepsilon_\mathrm{r} - j\sigma/(\omega\varepsilon_o)$ is the wedge complex relative permittivity, ε_r is the wedge relative permittivity, and σ is the wedge conductivity. The factor $H_{\mathrm{s,h}}$ is defined as [4]:

$$H_{\mathrm{s,h}} = R_{\mathrm{s,h}}(\alpha_0)\ R_{\mathrm{s,h}}(\alpha_n) \tag{5}$$

The soft and hard diffraction coefficients are given by Eq. (2a) in the following situations: when just one face, 0 or n, of the wedge is illuminated and the incidence angle $\phi_\mathrm{i} \leq n\pi/2$, where $n\pi$ is the wedge exterior angle (Fig. 1), or when both wedge faces are illuminated and the observer is between the two reflection boundaries. Otherwise, Eq. (2b) is used. The choice between Eqs. (2a) and (2b) is made to assure reciprocity, despite source and observer positions.

The definition of the angles α_0 and α_n, used in the Fresnel reflection coefficients, $R_{\mathrm{s,h}}(\alpha_{0,\mathrm{n}})$, is based on combinations of the angular definitions presented in [3–5, 7]. Luebbers' definitions for α_0 and α_n are [3]:

$$\alpha_0 = \min[\phi_\mathrm{i},\ n\pi - \phi_\mathrm{i}], \quad \alpha_n = \min[\phi_\mathrm{d},\ n\pi - \phi_\mathrm{d}] \tag{6}$$

where ϕ_i and ϕ_d are the directions of the incident and diffracted waves, respectively, both with respect to face 0 (Fig. 1). These angular definitions are also adopted in [4]. In [5], different angular definitions are proposed to ensure the reciprocity of Luebbers' heuristic coefficients:

TABLE 1 Angular Definitions for the Novel Heuristic Coefficients

Illuminated Face	α_0	α_n
Just face 0 $\phi_i \leq (n-1)\,\pi$	ϕ_i	$\begin{cases} \phi_d, & \phi_d < \pi - \phi_i \\ n\pi - \phi_d, & \text{otherwise} \end{cases}$
Just face n $\phi_i > \pi$	$n\pi - \phi_i$	$\begin{cases} \phi_d, & \phi_d \leq (2n-1)\pi - \phi_i \\ n\pi - \phi_d, & \text{otherwise} \end{cases}$
Both faces $(n-1)\pi < \phi_i \leq \pi$	$\min[\phi_i, n\pi - \phi_i]$	$\begin{cases} \phi_d, & \phi_d \leq \pi - \phi_i \\ n\pi - \phi_d, & \phi_d \geq (2n-1)\pi - \phi_i \\ \min[\phi_i, \phi_d,\ n\pi - \phi_i,\ n\pi - \phi_d], & \text{otherwise} \end{cases}$

$$\alpha_0 = \alpha_n = \min[\phi_i, \phi_d, n\pi - \phi_i,\ n\pi - \phi_d] \tag{7}$$

The angular definitions proposed in [7] take into account the transmitter and receiver locations. More specifically, they consider which wedge face is illuminated by the source and what is the receiver position relative to the shadow reflection boundaries.

Also considering the transmitter and receiver locations, this work proposes new definitions for α_0 and α_n, which are summarized in Table 1 and should be used with the novel heuristic coefficients defined by Eqs. (2a) and (2b). In principle, the novel diffraction coefficients preserve the characteristics of Holm's coefficients [4] except in regions where reflected rays are present, since Holm's coefficients do not work properly in such regions. In regions with reflected rays, new angular definitions are adopted to improve accuracy. When only one of the wedge faces, 0 or n, is illuminated, the angular definitions proposed in [7] are adopted. When both faces are illuminated, the angular definitios of [5] proved to be more appropriate.

3. SLOPE DIFFRACTION

In deep shadow regions, the observer is often obstructed in a way that only rays double diffracted by consecutive wedges reach the observer position, as illustrated in Figure 2. In this scenario, a first-order UTD alone will estimate null fields. Since the situation is important in the characterization of radio channels in urban environments, the application of diffraction coefficients of higher order will be considered. In that case, the slope diffraction, which is a second-order term of the UTD coefficients, is added to the first-order terms to yield the double diffracted field. Considering Figure 2 and following the procedure and considerations discussed in [3], the double diffracted electric field at the observer (considering first and second order diffracted fields) is given by:

$$E^{dd}(O) = \left(\frac{\overline{\overline{D_1}} \bullet \overline{\overline{D_2}}}{jks_2} \frac{\partial \overline{\overline{D_1}}}{\partial \phi_{d1}} \bullet \frac{\partial \overline{\overline{D_2}}}{\partial \phi_{i2}} \right) \bullet E^i(W_1) \sqrt{\frac{s_1}{(s_1+s_2)(s_2+s_3)}} e^{-jk(s_2+s_3)} \tag{8}$$

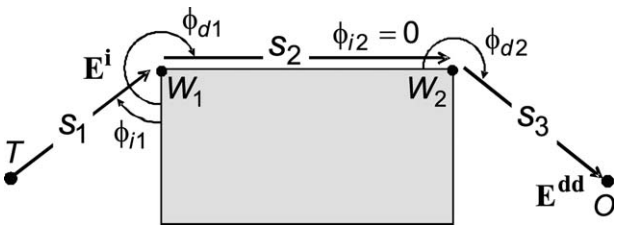

Figure 2 Double diffraction in consecutive wedges

where $\overline{\overline{D_1}}$ and $\overline{\overline{D_2}}$ are the dyadic diffraction coefficients relative to wedges W_1 and W_2, respectively, whose soft and hard heuristic elements are calculated from Eqs. (2a) and (2b).

To evaluate the partial derivatives of $\overline{\overline{D_1}}$ and $\overline{\overline{D_2}}$ in Eq. (8), it is necessary to define the partial derivatives of the diffraction coefficients with respect to ϕ_i and ϕ_d. For instance, the partial derivative of Eq. (2a) with respect to ϕ_i is given by (subscripts s and h are omitted):

$$\frac{\partial D}{\partial \phi_i} = G\left(\frac{\partial H}{\partial \phi_i} D_1 + H \frac{\partial D_1}{\partial \phi_i} + \frac{\partial R(\alpha_n)}{\partial \alpha_n} \frac{\partial \alpha_n}{\partial \phi_i} D_3 + R(\alpha_n) \frac{\partial D_3}{\partial \phi_i} + \frac{\partial D_2}{\partial \phi_i} + \frac{\partial R(\alpha_0)}{\partial \alpha_0} \frac{\partial \alpha_0}{\partial \phi_i} D_4 + R(\alpha_0) \frac{\partial D_4}{\partial \phi_i} \right) \tag{9}$$

The partial derivative with respect to ϕ_d has basically the same form of Eq. (9), with the appropriate sign inversions depending on which coefficient is being considered.

4. CASE STUDIES

4.1. Comparisons Among Different Heuristic UTD Coefficients

To demonstrate the usefulness of the proposed UTD formulation, the heuristic coefficients of [3–5, 7] and the novel heuristic coefficients proposed in Section 2 are compared to each other in the analysis of a right-angle ($n = 3/2$) lossy wedge illuminated by a normally incident plane wave. Both TM (soft) and TE (hard) polarizations are considered, and an accurate asymptotic diffractive analysis based on Maliuzhinets' coefficients [2] is adopted as reference for the comparative study. To account for losses, Maliuzhinets' coefficients were derived assuming a surface impedance over the wedge faces, meaning that no energy is transmitted to the wedge interior [2]. For both TM and TE polarizations, the directions of incidence $\phi_i = \pi/6$, $\pi/2$, and $3\pi/4$ are considered. The operation frequency is 1 GHz and observations are made 30λ away from the edge (i.e., $s_d = 30\lambda$), with $0 \leq \phi_d \leq 3\pi/2$ (Fig. 1). The lossy wedge has $\varepsilon_r = 10$ and $\sigma = 0.01$ S/m.

Figures 3–5 show the relative attenuation ($|E^d|/|E^i|$) and the absolute error with respect to the Maliuzhinets' solution, for $\phi_i = \pi/6$, $\pi/2$, and $3\pi/4$, respectively, and for both TM and TE polarizations. Table 2 summarizes the mean error and standard deviation with respect to Maliuzhinets' solution for each formulation, where all results of Figures 3–5 are considered. From Figures 3–5 and Table 2, one observes that the angular definitions proposed by Aïdi and Lavergnat [5] improve the results provided by Luebbers' heuristic coefficients [3]. For the results depicted in Figures 3–5, Holm's formulation [4] presents inaccuracies in the wedge lit regions, as expected. The results corresponding to the coefficients of [7] present inaccuracies and lack reciprocity for $\phi_i = \pi/2$ and $3\pi/4$ (Figs. 4 and 5, respectively). From Table 2 one observes that the smallest errors correspond to the novel heuristic coefficients, in average.

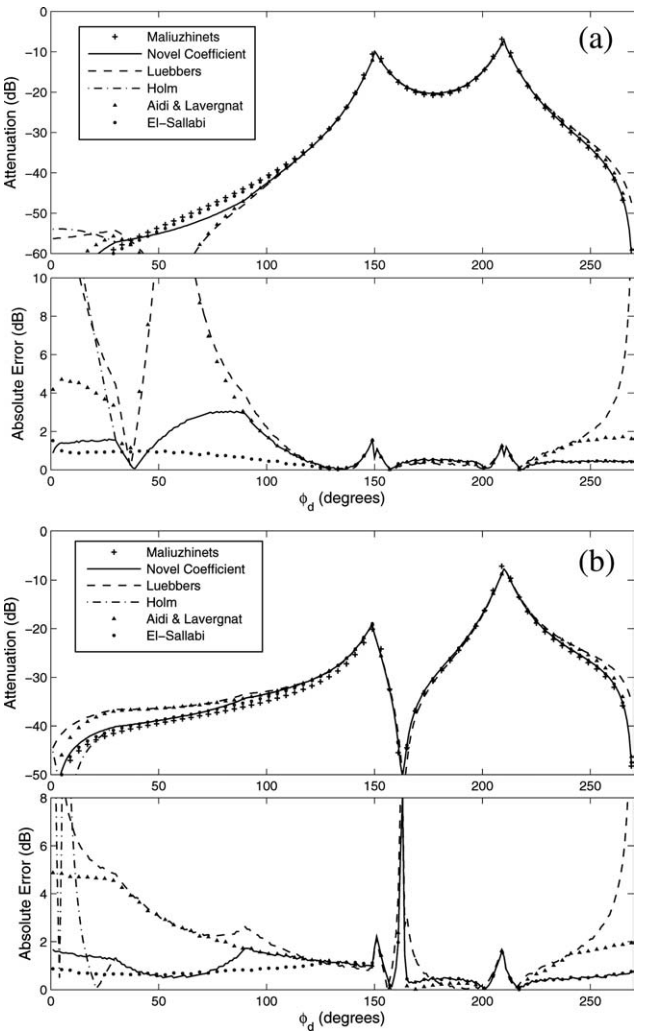

Figure 3 Attenuation of the field diffracted by the rectangular wedge for $\phi_i = \pi/9$ and corresponding error with respect to Maliuzhinet's solution: (a) TM and (b) TE polarizations

4.2. Simulations in an Urban-like Scenario

In the next case study, the wave propagation in a urban-like scenario is simulated. The scenario corresponds to the downtown core of Ottawa City, Canada. The plane view of the scenario is illustrated in Figure 6. Such scenario was already investigated in [9] and measured data are available for comparison purposes. Measurements were conducted at 910 MHz, using transmitting and receiving antennas with heights of 8.5 m and 3.65 m, respectively. In the numerical simulations, the transmitter is a vertical infinitesimal electric dipole (i.e., soft polarization with respect to the obstacle vertical wedges). To handle such scenario, a quasi-3D ray-tracing algorithm was implemented [10]. The algorithm considers reflections at ground and at obstacle surfaces. Neither reflections nor diffractions at the building tops are considered, as both transmitting and receiving antennas heights are much smaller than building's heights [9]. All ray paths from the transmitter (T) to the receivers (located along Laurier St. in Fig. 6) have a maximum of five reflections and two diffractions. Losses are considered assuming $\varepsilon_r = 7$ and $\sigma = 0.2$ S/m for reflections and diffractions at buildings, and $\varepsilon_r = 15$ and $\sigma = 0.05$ S/m for reflections at ground [10]. Slope diffraction is also considered in all simulations.

Figure 7 shows the path loss at the receiver locations, where results obtained by the heuristic formulation presented in Sections 2 and 3 are compared with measured data [9]. Results provided by other heuristic formulations [3–5, 7] are also presented in Figure 7. For a receiver close to the transmitter ($x < 600$ m), as the most relevant contributions come from reflections, all heuristic UTD formulations provide similar results, as summarized in Table 3. The differences between the UTD and measured results are probably due to the presence of vegetation [9], which was not considered in the simulations. In deep shadow regions ($x > 600$ m), the major contributions come from diffraction (i.e., single and double diffracted rays). From Table 3, one observes that for $x > 600$ m the results corresponding to the new heuristic UTD formulation and that of [5] provide slightly better results; but the statistical differences with respect other heuristic formulations are not significant.

5. CONCLUSIONS

This work presented novel heuristic UTD coefficients for the analysis of scattering by lossy wedges. The proposed coefficients combine features of previously investigated heuristic coefficients [3–5, 7] that not only make them reciprocal but also enhance their performance for arbitrary source and observer locations. Those properties enable the application of the novel heuristic

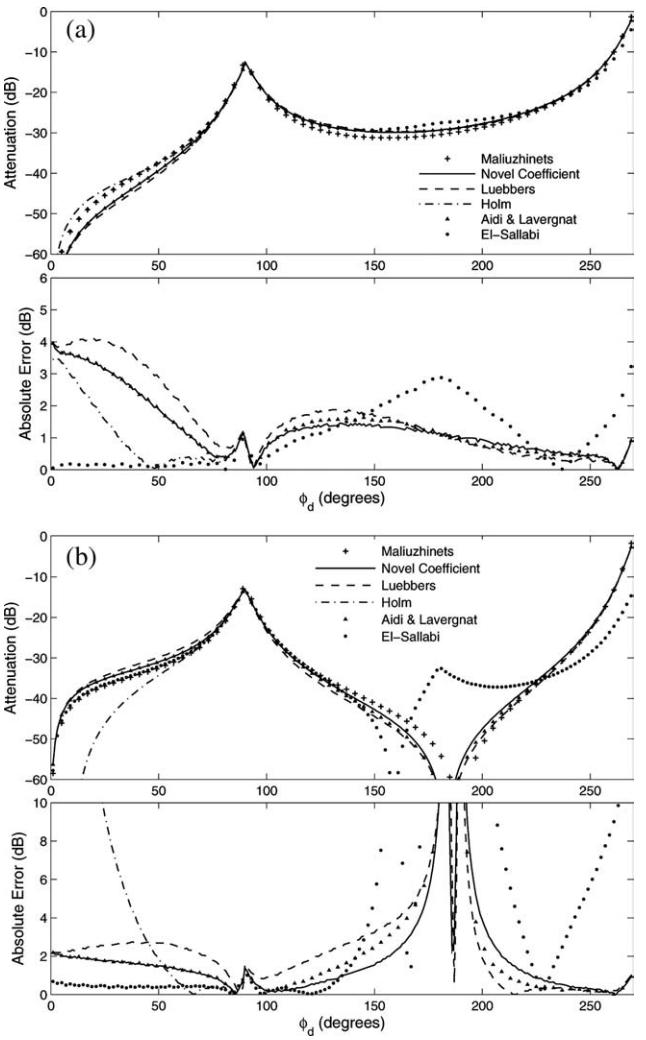

Figure 4 Attenuation of the field diffracted by the rectangular wedge for $\phi_i = \pi/2$ and corresponding error with respect to Maliuzhinet's solution: (a) TM and (b) TE polarizations

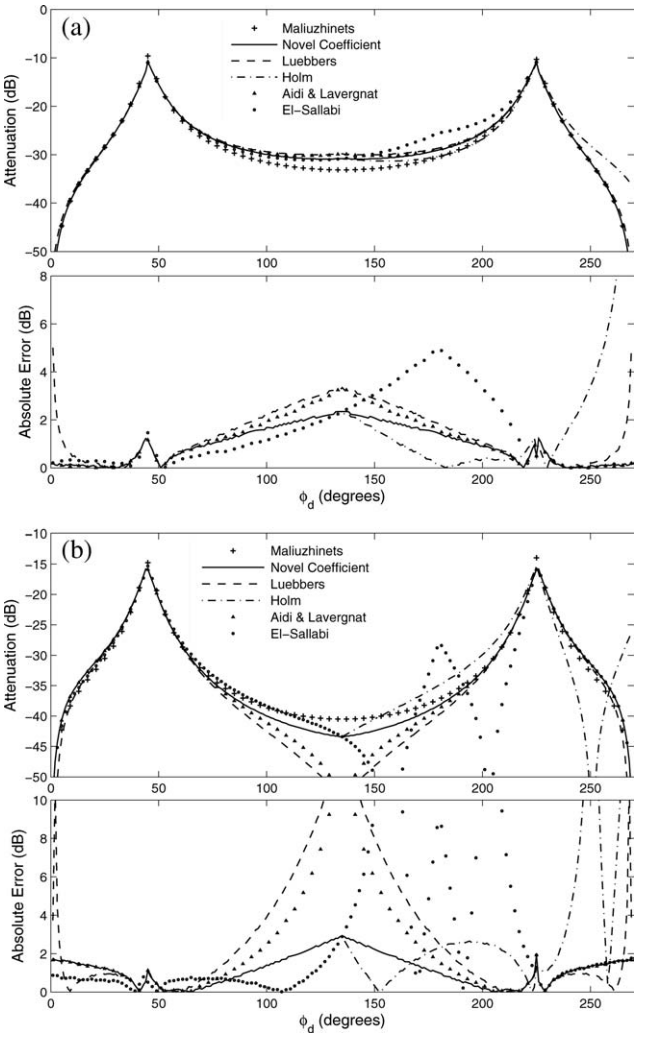

Figure 5 Attenuation of the field diffracted by the rectangular wedge for $\phi_i = 3\pi/4$ and corresponding error with respect to Maliuzhinet's solution: (a) TM and (b) TE polarizations

UTD coefficients in the characterization of radio channels in urban environments.

To validate the proposed heuristic coefficients, the scattering of a plane wave by a right-angle lossy wedge was analyzed. The novel coefficients, together with several other heuristic coefficients [3–5, 7], were compared against an accurate analysis based on the Maliuzhinets' diffraction coefficients [2], for both hard and soft polarizations and for different incident angles. The results demonstrated that, in average, the novel coefficients overcome innacuracies present in other formulations. Then, a real-life urban radio channel was characterized by the proposed

TABLE 2 Mean and Standard Deviation (SD) of the Absolute Error of the Simulations Shown in Figures 3–5 (Values in dB)

	TM Pol.		TE Pol.	
UTD	Mean	SD	Mean	SD
New coeff.	0.73	0.49	1.13	1.53
Luebbers	2.34	2.77	2.61	2.93
Holm	1.53	2.48	2.50	4.29
Aïdi	1.84	2.34	2.06	2.39
El-Sallabi	1.04	0.90	2.96	4.60

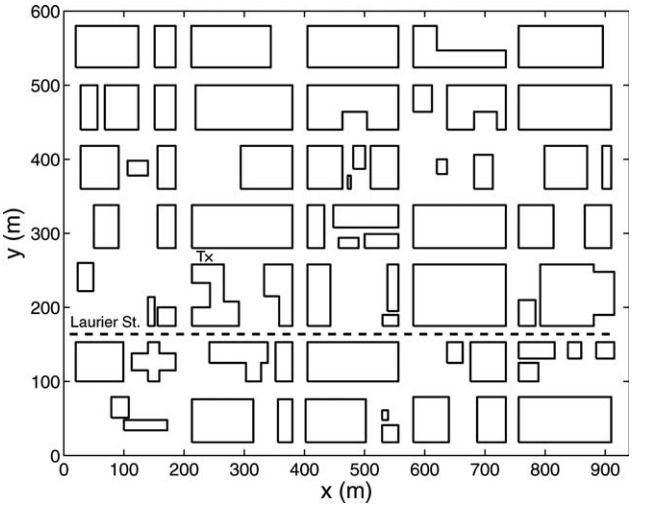

Figure 6 Plane view of the core region of Ottawa, Canada. Receivers located along Laurier St

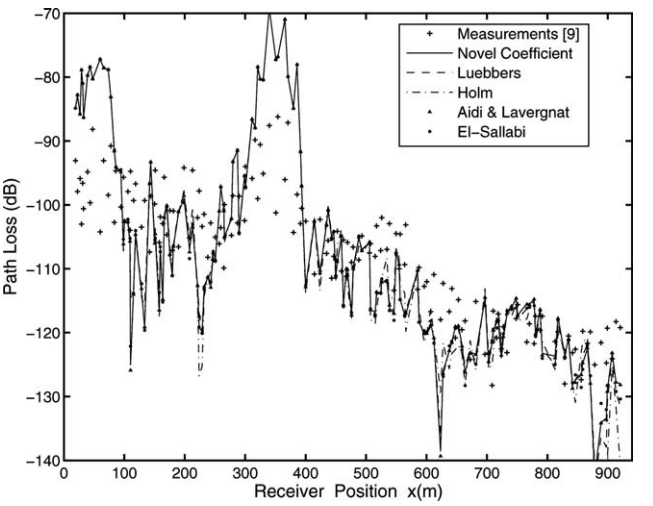

Figure 7 Path loss simulations for the scenario depicted in Figure 6

TABLE 3 Mean and Standard Deviation (SD) of the Absolute Errors of the Simulations Shown in Figure 7 (Values in dB)

	$x < 600$ m		$x > 600$ m	
UTD	Mean	SD	Mean	SD
New coeff.	9.11	6.33	5.46	4.45
Luebbers	9.08	6.31	5.66	4.82
Holm	9.05	6.48	6.71	6.62
Aïdi	9.10	6.32	5.51	4.54
El-Sallabi	9.08	6.23	5.70	5.83

heuristic UTD coefficients, with their performance compared against measurements [9]. All case studies illustrated and indicated the usefulness and applicability of the novel heuristic coefficients in the simulation of radiowave propagation in urban-like scenarios.

ACKNOWLEDGMENT

This work was partially supported by CNPq, CAPES, and FAPEMIG, Brazil.

REFERENCES

1. R. Kouyoumjian and P. Pathak, A uniform geometrical theory of diffraction for an edge in a perfectly conducting surface, Proc IEEE 62 (1974), 1448–1461.
2. T. Senior and J. Volakis, Approximate boundary conditions in electromagnetics, IEE Electromagn Wave Series, London, England, 1995.
3. R. Luebbers, A heuristic UTD slope diffraction coefficient for rough lossy wedges, IEEE Trans Antennas Propag 37 (1989), 206–211.
4. P. Holm, A new heuristic UTD diffraction coefficient for nonperfectly conducting wedges, IEEE Trans Antennas Propag 48 (2000), 1211–1219.
5. M. Aïdi and J. Lavergnat, Comparison of Luebbers' and Maliuzhinets' wedge diffraction coefficients in urban channel modelling, Progr Electromagn Res 33 (2001), 1–28.
6. P. Bernardi, R. Cicchetti, and O. Testa, A three-dimensional UTD heuristic diffraction coefficient for complex penetrable wedges, IEEE Trans Antennas Propag 50 (2002), 217–224.
7. H. El-Sallabi and P. Vainikainen, Improvements to diffraction coefficient for non-perfectly conducting wedges, IEEE Trans Antennas Propag 53 (2005), 3105–3109.
8. D. Schettino, F. Moreira, K. Borges, and C. Rego, Novel heuristic UTD coefficients for the characterization of radio channels, IEEE Trans Magn 43 (2007), 1301–1304.
9. J. Whitteker, Measurements of path loss at 910 MHz for proposed microcell urban mobile systems, IEEE Trans Vehicular Technol 37 (1988), 125–129.
10. D. Schettino, F. Moreira, and C. Rego, Efficient ray tracing for radio channel characterization of urban scenarios, IEEE Trans Magn 43 (2007), 1305–1308.

COUPLED-FED LOOP ANTENNA WITH BRANCH RADIATORS FOR INTERNAL LTE/WWAN LAPTOP COMPUTER ANTENNA

Kin-Lu Wong and Pei-Ji Ma
Department of Electrical Engineering, National Sun Yat-sen University, Kaohsiung 80424, Taiwan; Corresponding author: wongkl@ema.ee.nsysu.edu.tw

Received 21 March 2010

ABSTRACT: *A new antenna structure of internal long-term evolution/wireless wide area network (698–960/1710–2690 MHz) laptop computer antenna formed by a coupled-fed loop antenna connected with two branch radiators is presented. The two branch radiators consist of one longer strip and one shorter strip, both being efficient radiators and contributing multiresonant modes to greatly enhance the bandwidth of the antenna. The antenna's lower band is formed by a dual-resonant mode mainly contributed by the longer branch strip, while the upper band is formed by three resonant modes contributed respectively by one higher-order resonant mode of the longer branch strip, one resonant mode of the coupled-fed loop antenna alone, and one resonant mode of the shorter branch strip. The antenna's lower and upper bands can therefore cover the desired 698–960 and 1710–2690 MHz bands, respectively. The proposed antenna is suitable to be mounted at the top shielding metal wall of the display ground of the laptop computer and occupies a small volume of 4 × 10 × 75 mm^3 above the top shielding metal wall, which makes it promising to be embedded inside the casing of the laptop computer as an internal antenna. Details of the proposed antenna are studied in the paper.* © 2010 Wiley Periodicals, Inc. Microwave Opt Technol Lett 52:2662–2667, 2010; View this article online at wileyonlinelibrary.com. DOI 10.1002/mop.25556

Key words: *mobile antennas; internal laptop computer antennas; LTE antennas; WWAN antennas; coupled-fed loop antennas*

1. INTRODUCTION

To achieve dual-wideband operation to cover the long-term evolution (LTE) [1]/wireless wide area network (WWAN) [2] operation in the 698–960 MHz band for the LTE700/GSM850/900 operation and the 1710–2690 MHz band for the GSM1800/1900/UMTS/LTE2300/2500 operation is a design challenge for the internal laptop computer antennas. Recently, there have been promising internal laptop computer antennas reported for penta-band WWAN operation in the 824–960 and 1710–2170 MHz bands [3–10]. However, since the required bandwidths for the eight-band LTE/WWAN operation are much wider than the penta-band WWAN operation, especially in the lower band that mainly dominates the required dimensions of the antenna, the promising internal LTE/WWAN laptop computer antennas are still very few in the published papers [11]. In the reported design in Ref. 11, the internal eight-band LTE/WWAN laptop computer antenna occupies a volume of 4 × 10 × 85 mm^3 at the top edge of the display ground to cover the desired 698–960 and 1710–2690 MHz bands. Owing to the continuous requirement in decreasing the size of the internal antennas in the mobile devices, new antenna techniques in achieving smaller size of the internal laptop computer antennas are still very demanding.

In this article, a new antenna structure of internal laptop computer antenna formed by a coupled-fed loop antenna connected with two branch radiators for the eight-band LTE/WWAN operation in the laptop computer is presented. Owing to the proposed new antenna structure, which is different from the reported loop/monopole combo antenna [11] formed by combining a quarter-wavelength printed loop antenna with an internal matching circuit [12, 13] and a printed monopole antenna with an internal distributed inductor [14, 15] for the LTE/WWAN operation, the required size for covering the desired 698–960 and 1710–2690 MHz bands is 4 × 10 × 75 mm^3 only and is smaller than that of the reported antenna in [11]. Details of the proposed antenna are described in this article. The antenna are fabricated and tested, and the results of the fabricated antenna are discussed.

2. PROPOSED ANTENNA

Figure 1 shows the geometry of the proposed coupled-fed loop antenna with branch radiators for the eight-band LTE/WWAN operation in the laptop computer. In the study, the laptop computer is modeled as a display ground and a keyboard ground separated by an angle (α) of 90°. The two grounds are of the same dimensions of 200 × 260 mm^2, which is reasonable for practical laptop computers. The antenna is mounted at the shielding metal wall of width 5 mm and length 260 mm, which is connected to the top edge of the display ground to reduce possible coupling between the antenna and the circuitry on the back side of the laptop display. Also note that since the central region of the top edge of the display is mainly reserved to accommodate the lens of the embedded digital camera, the antenna is mounted along the top shielding metal wall with a spacing of 30 mm to the center line of the display ground.

The major portion of the antenna is printed on a 0.8-mm thick FR4 substrate of width 10 mm and length 75 mm. A 0.2-mm thick metal plate of size 4 × 75 mm^2 is then connected to the printed metal pattern on the FR4 substrate at point D, E, and F. The connected metal plate is orthogonal to the printed metal pattern and parallel to the shielding metal wall. The total volume of the antenna at the shielding metal wall is hence 4 × 10 × 75 mm^3, which is promising to be embedded inside the casing of the practical laptop computer.

The proposed antenna is mainly a coupled-fed loop antenna (path ADEC in the figure) with a longer branch strip (path EFG)